

Uniform Asymptotic Stability and Slow Convergence in Adaptive Systems

Benjamin M. Jenkins* **Travis E. Gibson*** **Anuradha M. Annaswamy***
Eugene Lavretsky**

* Department of Mechanical Engineering, Massachusetts Institute of Technology, Cambridge, MA, 02139 USA e-mail: (bjenkins@mit.edu).

** The Boeing Company, Huntington Beach, CA 92648 USA.

Abstract: We examine convergence properties of errors in a class of adaptive systems that arises for scalar plants. We show that these adaptive systems are at best uniformly asymptotically stable in the large, and possess an infinite region where the trajectories move arbitrarily slowly, i.e. *stick*. We show that these properties are also exhibited by adaptive systems with closed-loop reference models which have been demonstrated to exhibit improved transient performance. Despite such transient behavior, we show that the slow convergence can still occur and has the potential to be slower than classic open-loop reference model adaptive systems.

Keywords: Adaptive systems; Asymptotic stability; Convergence analysis

1. INTRODUCTION

Adaptive systems for the control of linear time-invariant plants can be shown to be stable under ideal conditions, with the tracking error converging to zero for any reference input. It is well known that if the conditions of persistence of excitation are met, then model reference adaptive control systems are uniformly asymptotically stable (u.a.s.) (Narendra and Annaswamy (2005)). One of the desirable properties however is exponential convergence as this ensures not only a fast convergence but also improved robustness. In this paper, we show that an inherent property exists in these standard adaptive systems that precludes such fast convergence, and that adaptive systems can only be shown to be globally u.a.s. and not exponentially stable. We also show that the implication of this property is that there is a region of slow convergence in the error space where the velocity of the underlying error state is finite and does not depend on its norm.

Recently, a new class of adaptive systems has been under discussion (see Lavretsky (2010), Gibson et al. (2012), Gibson et al. (2013), Stepanyan and Krishnakumar (2010)) which employ a closed-loop in the underlying reference model. These adaptive systems have a desirable transient response which leads to an improved tracking error whose L_∞ and L_2 norms are small compared to their open-loop counterparts. More importantly, the closed-loop signals such as the control input and control parameter have derivatives that have small magnitudes as well when compared to open-loop reference model systems. We also examine in this paper if the slow convergence that is present in the standard adaptive system with Open-Loop Reference models (ORM) is present in the Closed-Loop reference model (CRM)-based adaptive systems as well.

In order to provide an analytical insight into this sticking regime, we focus our attention in this paper on adaptive systems that arise for a first-order plant with a single unknown parameter. This allows us to quantify the underlying error system in

terms of second-order quadratic nonlinear differential equations for the ORM, and a third order system for the CRM case. We employ a qualitative theory of differential equations approach in order to identify a “sticking” region. We first analyze this region with the classical adaptive controller with a standard adaptive law, denoted as an ORM adaptive system. We then examine the effect of the closed-loop reference model on this sticking region. The regions in the ORM and CRM case are compared, using both qualitative theory of differential equations and numerical simulation studies.

2. THE CRM ADAPTIVE SYSTEM

Consider the scalar plant with an unknown parameter, a_p

$$\dot{x}_p(t) = -a_p x_p(t) + u(t) \quad (1)$$

with the controller defined by

$$u(t) = \theta(t)x_p(t) + r \quad (2)$$

where $\theta(t)$ is the time varying adaptive gain updated as

$$\dot{\theta}(t) = -\gamma e(t)x_p(t), \quad (3)$$

$e = x_p - x_m$, and x_m is the output of a reference model defined as

$$\dot{x}_m(t) = -a_m x_m(t) + r(t) + \ell(x_p(t) - x_m(t)). \quad (4)$$

ℓ in (4) is a feedback gain which introduces a closed-loop in the reference model. The error dynamics e then evolves by the following:

$$\dot{e}(t) = -a_L e(t) + \tilde{\theta}(t)x_p(t), \quad (5)$$

where $a_L = a_m + \ell$, $\tilde{\theta} = \theta - \theta^*$ and $\theta^* = -a_m + a_p$. Stability follows from the following Lyapunov function

$$V(e(t), \tilde{\theta}(t)) = \frac{e^2(t)}{2} + \frac{\tilde{\theta}^2(t)}{2\gamma}$$

with a derivative $\dot{V}(t) = -(a_m + \ell)e^2(t)$. Therefore $e, \tilde{\theta} \in \mathcal{L}_\infty$. This implies that $\dot{e} \in \mathcal{L}_\infty$. Integrating \dot{V} we can deduce

$$\|e(t)\|_{L_2}^2 \leq \frac{1}{a_m + \ell} V(e(0), \tilde{\theta}(0)). \quad (6)$$

* This work is supported by the Boeing University Strategic Initiative.

From Barbalat's Lemma $\lim_{t \rightarrow \infty} e(t) = 0$. If in addition, the reference input is non-zero, the persistence of excitation conditions are met and the system is u.a.s. The degree of persistence of excitation is not however only a function of r , but $e(0)$ and $\tilde{\theta}(0)$ as well.

The main benefit of CRM-adaptive systems is that ℓ can be increased independent from any other parameter in the system. This allows one to systematically reduce the L_2 norm of e as in (6) and increase the rate of decay of $V(t)$. This results in reduced chattering in the adaptive system, and when ℓ is chosen in conjunction with γ in an optimal fashion the adaptive system also portrays smooth transients in the control input (Gibson et al. (2012)). This, however, does not imply fast adaptation, as we will show in section 3. The introduction of a CRM results, in fact, in slower learning in the adaptive system as the reference model error has been artificially suppressed through the gain ℓ .

3. CONVERGENCE PROPERTIES OF THE ORM AND CRM ADAPTIVE SYSTEMS

In this section, we analyze the convergence properties of the ORM- and CRM-adaptive systems. Our attention is restricted to first-order plants with a single unknown parameter with a constant reference input. This simplest case is considered so as to clearly illustrate and quantify the convergence properties of the underlying nonlinear adaptive system. In both cases, we use the standard adaptive law as in Equation (3) without any robustness inducing modifications.

3.1 ORM

We start with equations (1)-(4) with $\ell = 0$, which defines the ORM-adaptive system. We set $r = r_0$, a positive constant, $x_m(0) = r_0/a_m$ so that

$$x_m(t) \equiv x_0 = \frac{r_0}{a_m} \quad \forall t \geq t_0 \quad (7)$$

Equation (7) is used in what follows in order to simplify the analysis. With (7), the ORM-adaptive system reduces to

$$\dot{e}(t) = -a_m e(t) + \tilde{\theta}(t)(e(t) + r/a_m) \quad (8)$$

$$\dot{\tilde{\theta}}(t) = -\gamma e(t)(e(t) + r/a_m) \quad (9)$$

The trajectories of (8) and (9) can therefore be fully characterized using a state-plane. Figure 1 illustrates a part of the state-plane, where the curves where $\tilde{\theta} = 0$ and $\dot{e} = 0$ are indicated. Also indicated are the vector field directions on these curves. As seen in the figure, the former occurs when $e = 0$ and $e = -x_0$, while the latter occurs on a parabola given by

$$S_{O4} = e_{Oh}(\tilde{\theta}) = \frac{\tilde{\theta}r}{a_m(a_m - \tilde{\theta})}.$$

It should be noted that the direction arrows are not drawn with lengths proportional to the state rate magnitude.

We now introduce a second hyperbola

$$e_{Oh2}(\tilde{\theta}) = 2e_{Oh}(\tilde{\theta}) - x_0 = \frac{r}{a_m} \frac{(a_m + \tilde{\theta})}{a_m - \tilde{\theta}} \quad (10)$$

which we will use to characterize certain invariance properties and speeds of the underlying trajectories.

Using these lines and hyperbolae, with

$$z = [e \ \tilde{\theta}]^T \in \mathbb{R}^2$$

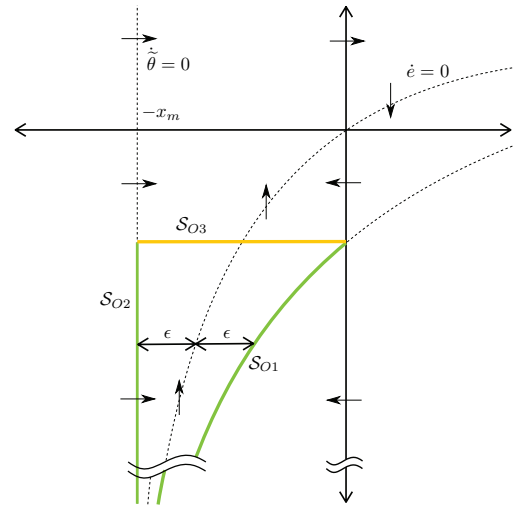


Fig. 1. M_O in $e, \tilde{\theta}$ space, with x_m held constant

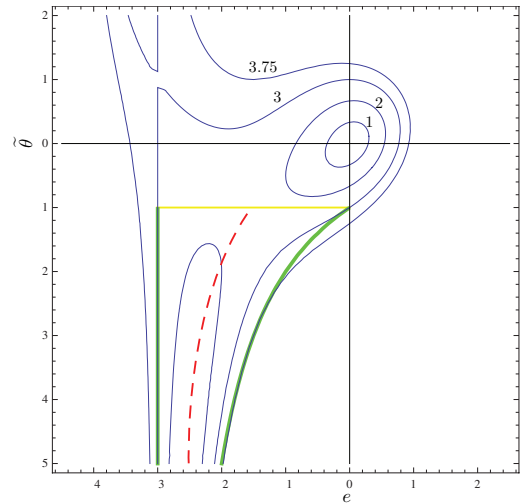


Fig. 2. Norm of state rate contours

we define a region, M_O as follows:

$$M_O : \left\{ z \mid \tilde{\theta} < -a_m, -\frac{r}{a_m} \leq e \leq \frac{r}{a_m} \frac{(a_m + \tilde{\theta})}{a_m - \tilde{\theta}} \right\}$$

M_O is indicated in Figure 1. As can be seen in the figure, M_O is bounded by the vertical lines $e = -x_0$ and the hyperbola $e_{Oh2}(\tilde{\theta})$ defined in equation (10), and extends in the $\tilde{\theta}$ -direction from $\tilde{\theta} = -a_m$ to $-\infty$. M_O is therefore an infinite region in the state-plane $(e, \tilde{\theta})$, bounded by the surfaces S_{O1} , S_{O2} , and S_{O3} .

$$S_{O1} : e(\tilde{\theta}) = \frac{r}{a_m} \frac{(a_m + \tilde{\theta})}{a_m - \tilde{\theta}}$$

$$S_{O2} : e = \frac{-r}{a_m}$$

$$S_{O3} : \tilde{\theta} = -a_m$$

We note that M_O is unbounded, since the hyperbola, S_{O1} is asymptotic to the line $e = -x_0$.

Figure 2 shows contours $\|z\| = c$ for

$$c = 1, 2, 3, 3.75$$

of an example with parameters of the adaptive system (1)-(4),

$$\begin{aligned} a_m &= 1, & \ell &= 0, & \gamma &= 1, \\ a_p &= 1, & \text{and} & & r &= 3 \end{aligned} \quad (11)$$

The region \mathbb{M}_O is superimposed on these contours. As can be seen from Figure 2, these contours are non-convex. It is also clear that $\|\dot{z}\| \leq 3.75$ at all points in \mathbb{M}_O . Theorem 1 is the analytical counterpart of this observation.

Theorem 1. Let

$$d_O = \frac{x_0^2 \gamma^2}{4}$$

Then

(i)

$$\|\dot{\tilde{\theta}}\| \leq d_O \quad \forall z \in \mathbb{M}_O \quad (12)$$

- (ii) all trajectories that start on \mathcal{S}_{O1} , and \mathcal{S}_{O2} enter \mathbb{M}_O ,
- (iii) once a trajectory enters \mathbb{M}_O at $t = t_0$ it will exit at $t = t_1 > t_0$ through \mathcal{S}_{O3} , and
- (iv) there exists a minimum time $T_1 = t_1 - t_0$ that all trajectories that start in \mathbb{M}_O will remain in \mathbb{M}_O which is given by

$$T_1 \geq \frac{|\tilde{\theta}(t_0)| - a_m}{d_O} \quad (13)$$

Proof. (i) Equation (12) is immediate from the definition of \mathbb{M}_O , and equation (3). That is, at all points in \mathbb{M}_O ,

$$\|\dot{\tilde{\theta}}\| \leq \frac{x_0^2 \gamma^2}{4} = d_O \quad \forall z \in \mathbb{M}_O \quad (14)$$

(ii) In order to evaluate the behavior of the trajectories on the surfaces \mathcal{S}_{O1} and \mathcal{S}_{O2} , we define normals \hat{n}_{O_i} to each surface \mathcal{S}_{O_i} , $i = 1, 2$. From the definitions of these surfaces it can be seen that

$$\hat{n}_{O2} = [1 \ 0]^T \quad (15)$$

Noting that a tangential vector on \mathcal{S}_{O1} is given by

$$\hat{t}_{O1} = \left[1 \ \left(\frac{\partial \tilde{\theta}}{\partial e} \right)_{S_{O1}} \right]^T$$

the normal vector that points into \mathbb{M}_O can be computed as

$$\hat{n}_{O1} = \left[- \left(\frac{\partial \tilde{\theta}}{\partial e} \right)_{S_{O1}} \ 1 \right]^T = \left[\frac{-2a_m x_o}{(x_o + e)^2} \ 1 \right]^T \quad (16)$$

It is therefore easy to see that

$$\hat{n}_{O_i}^T [\dot{z}]_{S_{O_i}} \geq 0, \quad i = 1, 2 \quad \forall z \in \mathbb{M}_O \quad (17)$$

The inequality (17) proves (ii).

(iii) The asymptotic stability of the ORM system shown in section 2 requires that all trajectories exit \mathbb{M}_O in order to reach $e = 0$. Equation (17) implies that any trajectory which exits \mathbb{M}_O must do so through \mathcal{S}_{O3} which proves (iii).

(iv) From (iii), we have that all trajectories starting at $z(t_0) = (e(t_0), \tilde{\theta}(t_0)) \in \mathbb{M}_O$ must traverse a distance of $|\tilde{\theta}(t_0)| - a_m$ in the $\tilde{\theta}$ -direction. From (i), we have that the maximum velocity of the trajectories in the $\tilde{\theta}$ -direction is d_O . Together, they imply that the trajectories spend a minimum time within \mathbb{M}_O of

$$T_1 \geq \frac{|\tilde{\theta}(t_0)| - a_m}{d_O}$$

which proves (iv). \blacksquare

Although not required for Theorem 1, it is useful for discussion to note that in \mathbb{M}_O not only is $\dot{\tilde{\theta}}$ finite, but \dot{z} is as well, with

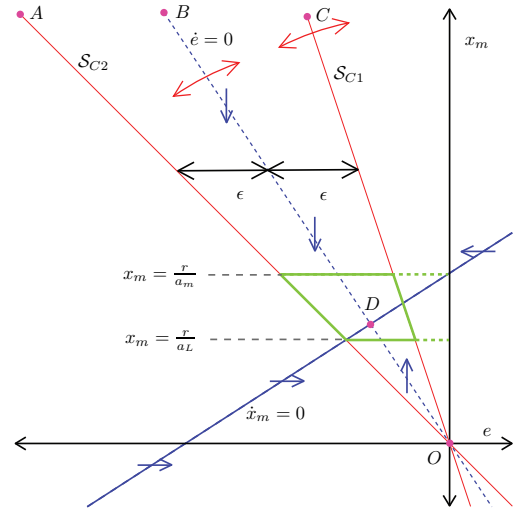


Fig. 3. \mathbb{M}_C in e, x_m space with $\tilde{\theta} \leq -a_L$. As $\tilde{\theta} \rightarrow -\infty$, OB and OC become OA . As $\tilde{\theta} \rightarrow -a_L$, OC aligns with the x_m axis. Point D is a local point of attraction.

$$\|\dot{z}\| \leq (r^2 + d_O^2)^{\frac{1}{2}} \quad \forall z \in \mathbb{M}_O$$

The main implication of Theorem 1 stems from (13). Noting that \mathbb{M}_O is an infinite region, and that it is possible to pick a $z_0 \in \mathbb{M}_O$ with $\|z_0\| > M$ for any finite M , it follows from (13) that T_1 can be made arbitrarily large. That is, the adaptive system can be "stuck" in this region \mathbb{M}_O for this large duration T_1 making it a "sticking regime".

Yet another implication is that this convergence period is a function of the norm $\|z(t_0)\|$ rather than the ratio of the starting and ending distances of z from the origin, which implies that the adaptive system is *NOT* exponentially stable.

3.2 CRM

We now turn our attention to equations (1) - (5) with $\ell \neq 0$, which is the CRM-based adaptive system. In this case, the underlying system is third order, and is given by

$$\begin{aligned} \dot{x}_m &= -a_m x_m + r + \ell e \\ \dot{e} &= -a_L e + \tilde{\theta}(e + x_m) \\ \dot{\tilde{\theta}} &= -\gamma e(e + x_m) \end{aligned}$$

Despite the higher order, we identify a region similar to \mathbb{M}_O with "sticking" properties. In addition to Figure 1, we can use Figure 3 to depict this region, denoted \mathbb{M}_C . With

$$z = [x_m \ e \ \tilde{\theta}]^T \in \mathbb{R}^3$$

this space \mathbb{M}_C is defined as

$$\mathbb{M}_C : \left\{ z \mid \tilde{\theta} < a_L, \frac{r}{a_L} \leq x_m \leq x_0, -x_m \leq e \leq \frac{x_m(a_L + \tilde{\theta})}{a_L - \tilde{\theta}} \right\}$$

where $x_0 = \frac{r}{a_m}$. \mathbb{M}_C is therefore a region in the state space $(x_m, e, \tilde{\theta})$, bounded by the surfaces \mathcal{S}_{C_i} , $i = 1, 2, 3, 4, 5$.

$$\mathcal{S}_{C1} : \quad e(\tilde{\theta}) = x_m \frac{(a_L + \tilde{\theta})}{a_L - \tilde{\theta}}$$

$$\mathcal{S}_{C2} : \quad e = -x_m$$

$$\mathcal{S}_{C3} : \quad x_m = \frac{r}{a_L}$$

$$\mathcal{S}_{C4} : \quad x_m = x_0$$

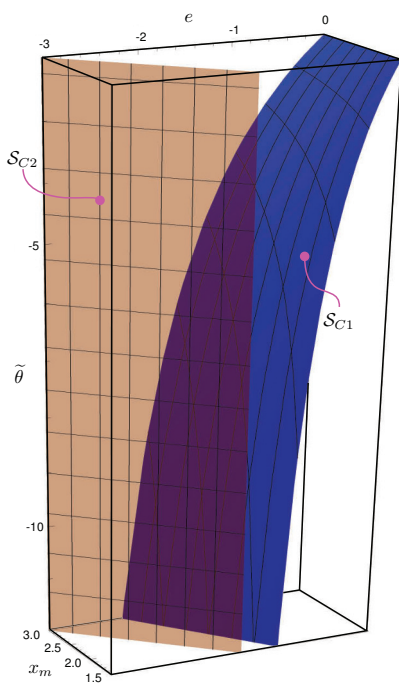


Fig. 4. 3D representation of \mathbb{M}_C for the example system defined in (11). In the figure, the front wall corresponds to S_{C3} , back wall to S_{C4} , and the ceiling to S_{C5} . The plane, denoted in tan color, corresponds to S_{C2} , and the hyperbolic surface, denoted in blue color, corresponds to S_{C1} . \mathbb{M}_C is the region bounded by S_{C5} on the top, and the surfaces S_{C1} and S_{C2} , but not bounded at the bottom, as both S_{C1} and S_{C2} extend to infinity in the $-\tilde{\theta}$ -direction. Therefore \mathbb{M}_C is an infinite region.

$$S_{C5} : \tilde{\theta} = -a_L$$

\mathbb{M}_C is unbounded since the hyperbolic surface S_{C1} is asymptotic to S_{C4} . A three dimensional representation is provided in Figure 4.

We now state the main result of this section in Theorem 2:

Theorem 2. (i)

$$\|\dot{\tilde{\theta}}\| \leq d_C \quad \forall z \in \mathbb{M}_C \quad (18)$$

where

$$d_C = \frac{\gamma x_0^2}{4}$$

- (ii) all trajectories that start on $S_{Ci}, i = 1, 2, 3, 4$ enter \mathbb{M}_C ,
- (iii) once a trajectory enters \mathbb{M}_C at $t = t_0$ it will exit at $t = t_1 > t_0$ through S_{C5} , and
- (iv) there exists a minimum time $T_1 = t_1 - t_0$ that all trajectories that start in \mathbb{M}_C will remain in \mathbb{M}_C which is given by

$$T_1 \geq \frac{|\tilde{\theta}(t_0)| - a_L}{d_C} \quad (19)$$

Proof. Equation (18) is immediate from the definition of \mathbb{M}_C and equation (3), that is, at all points in \mathbb{M}_C

$$\|\dot{\tilde{\theta}}\| \leq \frac{\gamma x_0^2}{4} = d_C \quad \forall z \in \mathbb{M}_C$$

- (ii) In order to evaluate the behavior of the trajectories on the surfaces $S_{Ci}, i = 1, 2, 3, 4$, we define normals \hat{n}_{Ci} to each surface S_{Ci} . From the definitions of these surfaces it can be seen that

$$\begin{aligned}\hat{n}_{C2} &= [1 \quad 1 \quad 0]^T \\ \hat{n}_{C3} &= [1 \quad 0 \quad 0]^T \\ \hat{n}_{C4} &= [-1 \quad 0 \quad 0]^T\end{aligned}$$

To define \hat{n}_{C1} , we select two unique tangential vectors on S_{C1} : $\hat{t}_{C1} = [1 \quad 0 \quad \left(\frac{\partial \tilde{\theta}}{\partial x_m}\right)_{S_{C1}}]^T$ and $\hat{t}_{C2} = [0 \quad 1 \quad \left(\frac{\partial \tilde{\theta}}{\partial e}\right)_{S_{C1}}]^T$. Therefore, \hat{n}_{C1} is given by

$$\hat{n}_{C1} = \hat{t}_{C1} \otimes \hat{t}_{C2}$$

where \otimes is the vector cross product operator. This results in

$$\hat{n}_{C1} = \left[\frac{2a_L e}{(x_m + e)^2} \quad \frac{-2a_L x_m}{(x_m + e)^2} \quad 1 \right]^T \quad (20)$$

It can be shown that,

$$\hat{n}_{Ci}^T [\dot{z}]_{S_{Ci}} \geq 0, i = 1, 2, 3, 4 \quad \forall z \in \mathbb{M}_C \quad (21)$$

The inequality (21) proves (ii).

- (iii) The asymptotic stability of the CRM system shown in section 2 requires that all trajectories from within \mathbb{M}_C exit \mathbb{M}_C in order to reach $e = 0$. Equation (21) implies that any trajectory which exits \mathbb{M}_C must do so through S_{C5} which proves (iii).

- (iv) From (iii), we have that all trajectories starting at $z(t_0) = (x_m(t_0), e(t_0), \tilde{\theta}(t_0))$ must traverse a distance of $|\tilde{\theta}(t_0)| - a_L$ in the $\tilde{\theta}$ -direction. From (i), we have that the maximum velocity of the trajectory in the $\tilde{\theta}$ -direction is d_C . Together, they imply that the trajectories spend a minimum time within \mathbb{M}_C of,

$$T_1 \geq \frac{|\tilde{\theta}(t_0)| - a_L}{d_C} \quad (22)$$

which proves (iv). \blacksquare

Although not required for Theorem 2 it is useful for discussion to note that not only is $\dot{\tilde{\theta}}$ finite, but \dot{z} is as well at all points in \mathbb{M}_C . The rates of each state within the region \mathbb{M}_C are,

$$\begin{aligned}\frac{-\ell r}{a_m} \leq \dot{x}_m &\leq \frac{\ell r}{a_L} \\ \frac{-a_L r}{a_m} \leq \dot{e} &\leq \frac{a_L r}{a_m} \\ 0 \leq \dot{\tilde{\theta}} &\leq \frac{\gamma r^2}{4 a_m^2}\end{aligned}$$

The above discussions clearly indicate that in the CRM-adaptive system, there is a region \mathbb{M}_C in the overall state space where $|\tilde{\theta}| - a_L$ can tend to infinity, but $\dot{\tilde{\theta}}$ remains finite. The discussions also indicate that all trajectories that start on the surfaces S_{C1} , S_{C2} , S_{C3} , and S_{C4} enter \mathbb{M}_C , and will leave only through the surface S_{C5} . Hence, \mathbb{M}_C is a "sticking region" where the system trajectories move with a finite velocity. Using the same arguments as above, we can conclude that the CRM-adaptive system is not exponentially stable as well.

3.3 Comparison of slow Convergence in the ORM and CRM

In order to compare the convergence properties described above, for the ORM- and CRM-adaptive systems, we define additional surfaces, S_{C6} where $\dot{x}_m = 0$ and S_{C7} where $\dot{e} = 0$

$$\mathcal{S}_{C6} : x_m(e) = x_0 + \frac{\ell}{a_m} e$$

$$\mathcal{S}_{C7} : e(x_m, \tilde{\theta}) = \frac{\tilde{\theta}x_m}{a_L - \tilde{\theta}}$$

True sticking occurs when both \dot{x}_m and \dot{e} are close to zero which occurs in the localized region where the solid and dotted blue lines meet in Figure 3. This can occur as low as $x_m = \frac{r}{a_L}$ and continue up to $x_m = \frac{r}{a_m}$. As sticking starts, the value of $\tilde{\theta}$ is well under its bound and actually closer to $\frac{\gamma r^2}{4 a_L^2}$. Yielding a result that the time rate of change of the adaptive parameter for the ORM and CRM deep (ie, $\tilde{\theta} \ll 0$) within \mathbb{M}_O or \mathbb{M}_C occurs on the order

$$\begin{aligned} \text{ORM} : \dot{\tilde{\theta}} &\sim \frac{\gamma r^2}{a_m^2} \\ \text{CRM} : \dot{\tilde{\theta}} &\sim \frac{\gamma r^2}{(a_m + \ell)^2}. \end{aligned} \quad (23)$$

This claim does not say that the CRM can never have faster convergence than the ORM system, but that there is a specific region in the state space where the performance of the CRM is significantly worse in terms of parameter convergence if the adaptive gain is not increased appropriately. Notice from (23) that the larger ℓ is made, the slower the parameter error converges. This claim is substantiated with simulations in the following section.

3.4 Sticking Regime and Projection Algorithm

Theorems 1 and 2 clearly indicate that the slow convergence is directly a function of $\tilde{\theta}(t_0)$. We also note that the adaptive laws employed in these adaptive systems are the standard ones and did not include any modifications. If, for instance, a projection algorithm is introduced, this puts a lower bound on T_1 in Theorems 1 and 2, with $\tilde{\theta}(t_0)$ replaced by θ_{max} , where θ_{max} is a known upper bound on θ (Lavretsky and Gibson (2011)). This implies, however, that the larger the θ_{max} , the slower the convergence properties.

We also note that in this paper, the reference input has been assumed to be a constant, and our focus has been on first-order plants with a single unknown parameter. A constant, non-zero, reference input is therefore persistently exciting and ensures parameter convergence. So the question that may be raised is if the sticking regime exists for general cases with an arbitrary reference input in a high-order plant. Recent results related to higher order adaptive systems indicate that these sticking regimes exist and are highly dependent on the persistence of excitation of the system.

4. SIMULATION EXAMPLES

Simulations are now presented with initial conditions starting within and on the edges of the “sticking” region, \mathbb{M}_O and \mathbb{M}_C , defined for the ORM- and CRM-adaptive systems respectively with parameters as defined in (11), with $\ell = 0$ for the ORM- and $\ell = 1$ for the CRM-adaptive system. 9 initial states are chosen specifically for each system, defined below in Tables 1 and 2. Rather than defining numerical values for each initial condition, we choose them as points of intersection of two unique surfaces indicated in Table 1. Similarly, the initial conditions for the CRM system are chosen as the points of intersection of

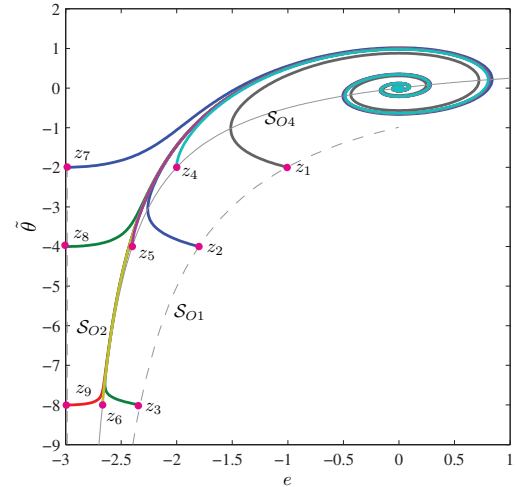


Fig. 5. 2D projection of the 3D state portrait for the ORM adaptive system with $a_m = 1, a_p = 1, \gamma = 1, r = 3$ and initial conditions defined in table 1

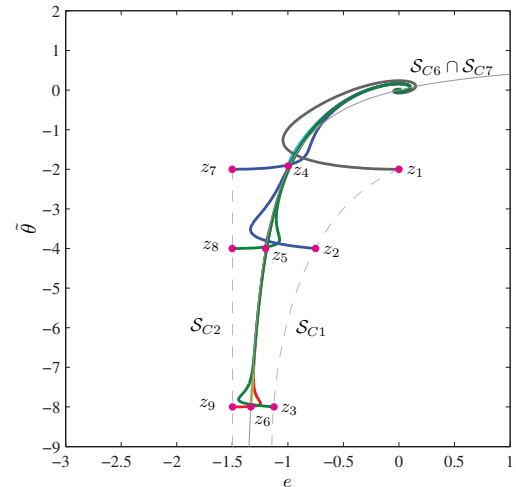


Fig. 6. 2D projection of the 3D state portrait for the CRM adaptive system with $a_m = 1, a_p = 1, \gamma = 1, \ell = 1, r = 3$ and initial conditions defined in table 2

three surfaces as indicated in Table 2. The algebra of solving for these points is straightforward and left to the reader. Figure

	\mathcal{S}_{O1}	\mathcal{S}_{O4}	\mathcal{S}_{O2}
$\tilde{\theta} = -2$	z_1	z_4	z_7
$\tilde{\theta} = -4$	z_2	z_5	z_8
$\tilde{\theta} = -8$	z_3	z_6	z_9

Table 1. Initial conditions $z_i, i = 1, 2, \dots, 9$ for the ORM example system. Each initial conditions, z_i , is the point of intersection of the two indicated surfaces in the corresponding row and column.

5 contains the 2-dimensional state portrait showing the state space trajectories of the ORM-adaptive system resulting from each of the initial conditions of Table 1. Also indicated in this figure is the surface \mathcal{S}_{O4} . Figure 6 contains the 2-dimensional projection of the 3-dimensional state space trajectories of the CRM-adaptive system resulting from each of the 9 initial conditions of Table 2. Also indicated in this figure is the projection of the curve $\mathcal{S}_{C6} \cap \mathcal{S}_{C7}$.

	\mathcal{S}_{C1}	\mathcal{S}_{C7}	\mathcal{S}_{C2}
$\tilde{\theta} = -2$	z_1	z_4	z_7
$\tilde{\theta} = -4$	z_2	z_5	z_8
$\tilde{\theta} = -8$	z_3	z_6	z_9

Table 2. Initial conditions $z_i, i = 1, 2, \dots, 9$ for the CRM example system. Each initial conditions, z_i , is the point of intersection of \mathcal{S}_{C6} and the two indicated surfaces in the corresponding row and column.

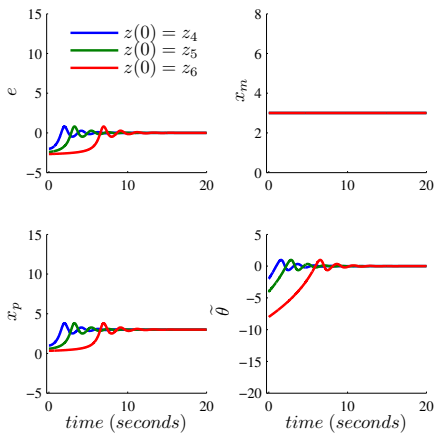


Fig. 7. Simulation of the the ORM adaptive system with $a_m = 1, a_p = 1, \gamma = 1, r = 3$ and initial conditions z_4, z_5, z_6 defined in table 1

Before we proceed to illustrate the sticking regime, we observe that in both Figures 5 and 6, there is an attractor that all initial conditions converge to. This attractor partially coincides with \mathcal{S}_{O4} in Figure 5 and $\mathcal{S}_{C6} \cap \mathcal{S}_{C7}$ in Figure 6. We focus on those initial conditions that are closest to these attractors that are common to both ORM- and CRM-adaptive, which are given by z_4, z_5 , and z_6 . With these initial conditions, we discuss the sticking regime in both adaptive systems.

We present time responses of $e, \tilde{\theta}, x_p$, and x_m for both the ORM- and CRM-adaptive systems in Figures 7 and 8, respectively, for the initial conditions z_4, z_5 , and z_6 for the same parameters in (11), with $\ell = 0$ and 1 for the ORM- and CRM-adaptive systems respectively. Introducing $\bar{z}(t) = z(t) - z(t_\infty)$ and defining T_s as the settling time beyond which $\|\bar{z}(t)\|$ reduces to 5% of its initial value, we see that, $T_s = 5.37s, 5.62s, 8.19s$ for these three initial conditions for the ORM-system and $T_s = 3.69s, 5.85s, 12.74s$ for the CRM-system. Notice that although $\frac{\bar{z}(t_0)}{\bar{z}(t_0+T_s)}$ is identical for all three trajectories, T_s increases unbounded as $\|\bar{z}(t_0)\|$ increases, implying that the system is not exponentially stable. The sticking characteristic is obvious from the flat portion exhibited by e and x_p for initial conditions z_5 and z_6 in both figures prior to convergence.

Trajectories initialized at both z_5 and z_6 demonstrate the "sticking" property described in this paper, which is characterized by the nearly flat portion of the response of e and x_p prior to convergence. From the third initial condition, z_6 , the exacerbated sticking effect in the CRM-adaptive system can clearly be seen. Even with a feedback gain of $\ell = 1$ the error convergence for large initial conditions is even slower compared to that of the ORM-system. It was observed that this convergence became

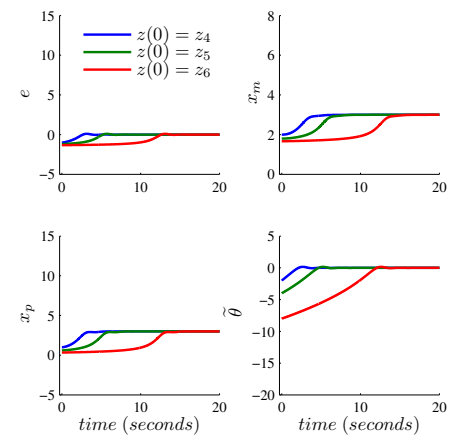


Fig. 8. Simulation of the the CRM adaptive system with $a_m = 1, a_p = 1, \gamma = 1, r = 3$ and initial conditions z_4, z_5, z_6 defined in table 2

slower as ℓ was increased further. It should be noted that these convergence properties co-exist with the absence of the oscillatory behavior in the CRM in comparison to the ORM. That is, the introduction of the feedback gain ℓ helps in producing a "smooth" adaptation, but not a fast adaptation.

5. CONCLUSIONS

This work illustrates the convergence properties of a class of adaptive systems with scalar plants. Using a qualitative theory of differential equations we show that, even when the persistence of excitation conditions on the input are satisfied, the convergence is at most uniformly asymptotic and not exponential. This arises from the existence of an infinitely large region where the trajectories may move arbitrarily slowly due to the system dynamics decreasing the degree of persistence of excitation. In this work it is also shown that while CRM adaptive systems show improved transient performance in terms of a reduced \mathcal{L}_2 norm in the tracking error, parameter error convergence can be potentially slower than the ORM counterpart.

REFERENCES

- Gibson, T.E., Annaswamy, A.M., and Lavretsky, E. (2012). Closed-loop reference model adaptive control: Stability, performance and robustness. *IEEE Trans. Automat. Contr. (submitted)*.
- Gibson, T.E., Annaswamy, A.M., and Lavretsky, E. (2013). Closed-loop Reference Model Adaptive Control, Part I: Transient Performance. In *American Control Conference (submitted)*.
- Lavretsky, E. (2010). Adaptive output feedback design using asymptotic properties of lqg/ltr controllers. In *AIAA 2010-7538*.
- Lavretsky, E. and Gibson, T.E. (2011). Projection operator in adaptive systems. *arXiv e-Prints*, arXiv:1112.4232.
- Narendra, K.S. and Annaswamy, A.M. (2005). *Stable Adaptive Systems*. Dover.
- Stepanyan, V. and Krishnakumar, K. (2010). Mrac revisited: guaranteed performance with reference model modification. In *American Control Conference*.